Biomedicine & Pharmacotherapy 168 (2023) 115682

Contents lists available at ScienceDirect

Biomedicine & Pharmacotherapy

journal homepage: www.elsevier.com/locate/biopha

Antiviral, virucidal and antioxidant properties of *Artemisia annua* against SARS-CoV-2

Melissa Baggieri [a,1], Silvia Gioacchini [a,1], Gigliola Borgonovo [b], Giorgia Catinella [b], Antonella Marchi [a], Pasquale Picone [c], Sonya Vasto [c,d], Raoul Fioravanti [a], Paola Bucci [a], Maedeh Kojouri [a], Roberto Giuseppetti [a], Emilio D'Ugo [a], Fausto Ubaldi [e], Sabrina Dallavalle [b], Domenico Nuzzo [c], Andrea Pinto [b], Fabio Magurano [a,*]

[a] Istituto Superiore di Sanità, Dipartimento di Malattie Infettive, Viale Regina Elena 299, 00161 Roma, Italy
[b] Dipartimento di Scienze per gli Alimenti, la Nutrizione e l'Ambiente, DeFENS, Università degli Studi di Milano, Via Celoria 2, 20133 Milano, Italy
[c] Istituto per la Ricerca e l'Innovazione Biomedica, Consiglio Nazionale delle Ricerche, Via U. La Malfa 153, 0146 Palermo, Italy
[d] Dipartimento di Scienze Biologiche, Chimiche, Farmaceutiche e Tecnologiche, STEBICEF, Università degli Studi di Palermo, Viale delle Scienze, 90128 Palermo, Italy
[e] Merck Serono S.p.a., Roma 00176, Roma, Italy

ARTICLE INFO

Keywords:
COVID-19
SARS-CoV2
Antiviral
Artemisia annua
Antioxidant activity
Artemisinic acid

ABSTRACT

Natural products are a rich source of bioactive molecules that have potential pharmacotherapeutic applications. In this study, we focused on Artemisia annua (A. annua) and its enriched extracts which were biologically evaluated in vitro as virucidal, antiviral, and antioxidant agents, with a potential application against the COVID-19 infection. The crude extract showed virucidal, antiviral and antioxidant effects in concentrations that did not affect cell viability. Scopoletin, arteannuin B and artemisinic acid (single fractions isolated from A. annua) exerted a considerable virucidal and antiviral effect in vitro starting from a concentration of 50 μg/mL. Data from Surface Plasmon Resonance (SPR) showed that the inhibition of the viral infection was due to the interaction of these compounds with the 3CLpro and Spike proteins of SARS-CoV-2, suggesting that the main interaction of compounds may interfere with the viral pathways during the insertion and the replication process. The present study suggests that natural extract of A. annua and its components could have a key role as antioxidants and antiviral agents and support the fight against SARS-CoV-2 variants and other possible emerging Coronaviruses.

1. Introduction

The COVID-19 pandemic caused by Severe Acute Respiratory Coronavirus 2 (SARS-CoV-2) remains a global emergency. The World Health Organization reported that in the 28 days between 23 January and 19 February 2023, nearly 5.3 million new cases and over 48 000 deaths were reported globally [1].

At the beginning of the pandemic, no specific and effective antiviral drugs were available to treat the disease. Chloroquine, hydroxychloroquine, remdesivir, and lopinavir/ritonavir were highlighted as repurposed drugs that could treat COVID-19, by acting on specific viral enzymes or the replication cycle. The antimalarial drug chloroquine and its derivative hydroxychloroquine was found to efficiently inhibit SARS-CoV-2 in vitro [2]. This raised an interesting question among scientists of whether other antimalarial drugs also have anti-SARS-CoV-2 potential. Moreover, since natural compounds and phytochemical treatments had been used successfully to treat coronavirus infections during the SARS-CoV and MERS-CoV outbreaks, and the fact that several conventional drugs failed against viral infections, plant extracts have been viewed as a valuable source of therapeutically relevant products [3–7]. The identification of natural molecules that are able to counteract virus replication, inflammation, and oxidative stress represents a new medical challenge [4–6,8,9].

Artemisia annua (*A. annua)* is a medicinal plant that belongs to the Asteraceae family and is widely distributed throughout temperate zones. This herb has been traditionally used to treat fever and malaria [10-13]. The main bioactive compounds of *A. annua* are sesquiterpene lactones, monoterpenes, triterpenoids, steroids, and flavonoids [14]. The

* Corresponding author.
E-mail address: fabio.magurano@iss.it (F. Magurano).
[1] These authors equally contributed to the work

https://doi.org/10.1016/j.biopha.2023.115682
Received 17 July 2023; Received in revised form 6 October 2023; Accepted 8 October 2023
Available online 11 October 2023

principal sesquiterpene of *A. annua* is artemisinin. Artemisinin, named *quinghaosu* in China, is a polycyclic sesquiterpene lactone that has a peroxide function. The artemisinin derivatives, collectively called "artemisinins", include artesunate, dihydro-artemisinin, artemether, arteannuin B, and artemisone, among others. These compounds have been reported to be involved in several activities with important pharmacological applications, including the treatment of malaria, Rheumatoid Arthritis (RA), Systemic Lupus Erythematosus (SLE), and allergic contact dermatitis [15]. Recently, *A. annua* gained increasing attention thanks to its anticancer properties [16]. Today, the World Health Organization (WHO) recommends Artemisinin-based Combination Therapy (ACT) as the first-line treatment for uncomplicated multi-drug-resistant malaria [17,18]. Moreover, the antiviral broad-spectrum potential of artemisinin has been demonstrated in several studies against a wide range of DNA and RNA viruses, including.

Human CytoMegaloVirus (HCMV), Human Herpes Simplex Virus (HSV), Hepatitis B Virus (HBV), Hepatitis C Virus (HCV), Human Immunodeficiency Virus (HIV), Polyomavirus BK and Zika Virus [19-21].

Hopes regarding the use of artemisinin as a potential treatment for COVID-19 are largely based on a paper published by Chinese scientists, who screened 200 medicinal herbs to study their effect on the coronavirus that caused the outbreak of SARS in 2002–2003 [22]. *A. annua* was found to be the second most effective of the herbs tested, after *Lycoris radiata*. Preliminary results of a study conducted in vitro on the SARS-CoV-2 infection in permissive cells demonstrated the efficacy of artemisinin and its derivatives through pre-treatments and infection treatments on different cell models. [23,24]. Moreover, the potential of artemisinin against SARSCoV-2 was also confirmed by a study [25] that evaluated the activities of nine artemisinin-related anti-SARS-CoV-2 compounds in vitro, establishing a pharmacokinetic model that can predict the therapeutic potential of selected compounds against SARS-CoV-2.

Recently, Nair and colleagues [26] measured the antiviral activity of dried leaf aqueous extracts of seven cultivars of *A. annua* from the four continents. Hot-water leaf extracts based on artemisinin showed antiviral activity with IC_{50} values of 0.1–8.7 μM. Artemisinin alone was less active with an IC_{50} value that was eightfold greater (about 70 μM), suggesting that the plant extracts are more potent than the single compounds against SARS-CoV-2, probably due to a synergistic action that blocks viral infection post-entry. These results were also confirmed by studies extended to the other main variants of SARS-CoV-2 that appeared later [27,28].

In silico studies have been recently performed to investigate the inhibition of the coronavirus-host protein interaction by *A. annua* single components. In particular, molecular docking studies have revealed that artemisinin is able to inhibit the binding of the spike protein to cell surface receptors, thus potentially preventing both the endocytosis of the virus and the activation of the NF-kB signalling pathway (Cao et all., 2020; [29-31]). In another recent in silico study, Ikanovic, and coworkers [32] examined the interaction of scopoletin, a coumarin isolated from artemisia species and other plants (*Scopolia japonica* Maxim. - Japanese belladonna, *Artemisia scoparia* Waldst. & Kit. - wormwood and *Viburnum prunifolium* L. - black haw), with the main protease Mpro SARS-CoV-2. The docking analysis showed that scopoletin has a significant binding affinity (−6.9 kcal/mol) for the SARS-CoV-2 main protease, supporting its potential use in the fight against COVID-19.

In addition to compounds with potential antiviral activity, the profiles of secondary metabolites in *A. annua* highlighted a relevant level of antioxidant molecules in the leaves [33]. These findings are relevant given that the major complications afflicting people during and after COVID-19 are attributable to oxidative stress, which occurs due to an imbalance between the formation and neutralization of free radicals during SARS-CoV-2 infection [34-36]. Damage caused by the excessive production of reactive oxygen species (ROS), such as an inadequate antioxidant response and increased lipid peroxidation, leads to infectious diseases and viral replication. In this scenario, the antioxidant components of *A. annua* may support the antiviral activity and counteract the inflammatory response in COVID-19 [37].

In the present work, we focused on obtaining and chemically characterizing *A. annua* enrichedextracts, which were biologically evaluated in vitro as virucidal, antiviral, and antioxidant agents, with a potential application against the COVID-19 infection.

2. Material and methods

2.1. Chemicals and equipment

All solvents were purchased from Merck Life Science (Milan, Italy). Analytical TLC was conducted on TLC plates (silica gel 60 F254, aluminum foil) and the spots were detected under UV light at 254 nm or were revealed by a solution of anisaldehyde (2%) and sulphuric acid (2%) in EtOH. NMR spectra were recorded on a Bruker Avance 600 MHz spectrometer. High-Resolution Preparative HPLC was performed with a C-18 Ascentis, Supelco (21.2 mm i.d., 250 mm, 5 μm), fitted to a 1525 Extended Flow Binary HPLC pump and a Waters 2489 UV–Vis detector (both from Waters, Milan, Italy).

2.2. Extraction and purification methods

The *A. annua* extract was obtained from a private cultivation in the province of Spoleto, Umbria, Central Italy. Briefly, a crude plant extract was prepared from leaves harvested at pre-flowering stage, as follows: 800 g of fresh leaves were soaked in 1 L of 96% ethanol, so that all leaves were in contact with the alcohol, and incubated in the dark at room temperature. After 5 days, this mother tincture was filtered through cotton wool. 10 mL of tincture were evaporated at room temperature under a flow of nitrogen to obtain 590 mg of crude extract. Then, the residue obtained was dissolved in 10 mL of water and extracted three times with ethyl acetate. The organic phase was separated, dried on dry sodium sulphate and evaporated until dry under reduced pressure to produce 106 mg of crude extract. A stock solution of 9.4 mg/mL was prepared by dissolving the ethyl acetate residue in methanol.

The solution was filtered using a nylon syringe filter of 0.45 μm and analysed by analytical HPLC.

For the separation of the compounds, a preparative HPLC was used. A stock solution of the extract (9.4 mg/mL) was separated with the elution gradient consisting of eluent A (water) and eluent B (ACN). The initial conditions were: 50% eluent B followed by a linear gradient over 20 min, then 100% of B until 30 min. The flow rate was 15 mL/min, the volume of injection 1 mL. The detector was set at 210 nm.

The fractions corresponding to the major peaks, F1-F8 (Fig. 2, Table 1), were collected and the solvent was removed in vacuo. Structures of the molecules were identified by 1D and ^{2}D NMR by comparison with reference data from literature.

2.3. A549 cell culture and treatment

Epithelial A549 lung cancer cell lines (ATCC® CCL-185IG™) were cultured with the Roswell Park Memorial Institute (RPMI) 1640 medium and supplemented with 10% fetal bovine serum (FBS), 100 U/mL penicillin, and 100 U/mL streptomycin (Sigma) and 2 mM L-glutamine in a humidified atmosphere of 95% air and 5% CO_2 at 37 °C. The cells were treated with 25, 50, 100, and 200 μg/mL of *A. annua* extract, 65, 125, 250, and 500 μM of the oxidative agent *tert*-butyl hydroperoxide (TBH, Luperox® TBH70X, Merck Life Science S.r.l., Italy) for 24 h, alone and in combination, to analyse cell viability and evaluate morphology, and for 2 h, for an ROS assay. The control (Ctrl) groups received an equal volume of the solvent medium.

2.4. Cell morphology

Cell morphology was measured by tracing the surface of the cell

Table 1
^{1}H chemical shift of isolated compounds in the *A. annua* extract.

Isolated fraction	Retention time Rt, min	Weight of fraction, mg	Substance/class of metabolites	^{1}H chemical shift, δ in ppm, (multiplicity)	references
F1	2702,3.515 (several peaks)	14.3	Mixture of unidentified compounds	-	-
F2	4724	2.3	Scopoletin	3.91 (s), 6.77 (s), 6.28 (d), 7.84 (d), 7.11 (s)[a]	[38]
F3	7947	3.0	Mixture of compounds, the main components are flavonoids	Several singlets at 3.8–4.0 ppm, aromatic protons between 5.6 and 7.8 ppm	-
F4	13,299	3.3	Chrysoplenetin	3.84, 3,93, 3.95 and 3.98 (four s), 6.48 (s), 7.05 (d), 7.64–7.75 (m)	[39]
F5	19,742	1.8	Arteannuin B	0.98 (d), 1.3–2.1 (m), 2.73 (m), 2.68 (s), 5.42 (d), 6.15 (d)	[39]
F6	24,315	1.4	Artemetin (+ isomer)	3.87, 3.91, 3.97, 3.97 and 3.98 (five s), 6.50 (s), 6.9–7.8 (m), 8.57 (s)	Kontogiani et al., 2019
F7	30,552	1.7	Mixture of terpenoids	Several signals in all spectrum	-
F8	32,473	3.0	Artemisinic acid	0.95 (d), 1.0–2.0 (m), 2.60, 2.68 (ddd), 4.98 (bs), 5.55 (s), 6.44 (s)	[39]

[a] MeOH-d4.

using ImageJ 1.52 v software (National Institutes of Health, Bethesda, Maryland, USA). The average value of the cellular body was used for statistical analysis using GraphPad Prism 8.4.3 software (Northside Dr, San Diego, CA, USA).

2.5. Vero E6 cells and virus propagation

The permissive cells, named Vero E6 clone 1008, (Cercopithecus aethiops derived epithelial kidney,

ATCC# 1586) were grown and maintained in Minimum Essential Medium (MEM + GlutaMAX, Gibco), supplemented with 10% fetal bovine serum (FCS), 100 U/mL penicillin, 100 U/mL streptomycin, 1 mM sodium pyruvate, and 1% non-essential amino acids, at 37 °C in 5% CO_2.

The viral BetaCov/Italy/CDG1/2020|EPI ISL 412973|2020–02–20 isolate (GISAID accession ID: EPI_ISL_412973) was propagated through the inoculation of 70–80% confluent Vero E6 cells. Cells were observed for their cytopathic effect (CPE). Stocks of SARS-CoV-2 virus were harvested at 72 h post infection (p.i.), and supernatants were collected, clarified, aliquoted, and stored at − 80 °C. The virus titer was determined as Plaque Forming Units (PFU/mL). This strain had a viral titer of $10^{7.9}$ $TCID_{50}$/mL. Virus propagation and all virus manipulation were conducted under biosafety level-3 facility at the Istituto Superiore di Sanità in Rome.

2.6. Cytotoxicity assays

The A549 cells were grown at a density of 2×10^4 cells/well on 96-well plates in a volume of 100 μL/well. After treatment, cell viability was assessed by MTS assay (Promega Italia S.r.l., Milan, Italy) by absorbance measurements at a wavelength of 490 nm, after 2 h incubation at 37 °C. Cell viability was expressed by normalization with the control. For the analysis of cell morphology, the cells were washed twice with PBS and cellular images were obtained using the Zeiss Axio Scope 2 microscope (Carl Zeiss, Oberkochen, Germany).

The Vero E6 cells were grown at a density of 1×10^4 cells/well in 96-well plates and treated for 24 h with the *A. annua* extract (from 1000 to 10 μg/mL), the EtOAc fraction (from 1000 to 10 μg/mL) and its main isolated components (F1-F8) (from 100 to 1 μg/mL). Then, an XTT (Cell Proliferation Kit II, Roche) assay was performed as previously described [4,5]. The measured absorbance directly correlates with the number of viable cells.

2.7. Virucidal activity by plaque reduction neutralization test

The Plaque Reduction Neutralization Test (PRNT) assay was used to assess the virucidal potential of the *A. annua* extract against SARS-CoV-2, as previously described [4,5]. The extract was resuspended in 30% dimethyl sulfoxide (DMSO) leading to a final concentration of 100 mg/mL, which did not affect the growth of the cells in vitro. Then, serial 10-fold dilutions of the extract (from 0.05 mg/mL to 0.0005 μg/mL) were incubated with 80 PFU of SARS-CoV-2 at 4 °C overnight (~16 h). The mixtures were added in triplicate to confluent monolayers of Vero E6 cells, grown in 12-well plates and incubated at 37 °C in a humidified 5% CO_2 atmosphere for 60 min 4 mL/well of a medium containing 2% Gum Tragacanth + MEM 2X supplemented with 2.5% of heat inactivated FCS was added. The plates were left at 37 °C with 5% CO_2. After 3 days, the overlay was removed, and the cell monolayers were washed with PBS to completely remove the overlay medium. The cells were stained with a crystal violet 1.5% alcoholic solution. The presence of SARSCoV-2 infected cells was indicated by the formation of plaques. The half-maximal inhibitory concentration (IC_{50}) was determined as the highest dilution of the substance resulting in a 50% ($PRNT_{50}$) reduction of plaques compared to the virus control, and it was calculated using the GraphPad Prism software. Through this method, the *A. annua* extract (from 500 to 0.0005 μg/mL),

EtOAc fraction (from 500 to 0.0005 μg/mL), water fraction at 50 μg/mL and single bioactive fractions (50 μg/mL) were tested.

2.8. Antiviral activity

The Vero E6 cells were seeded in 24-well plates at a concentration of 200,000 cells/well and incubated at 37 °C in a humidified 5% CO_2 atmosphere. After 24 h, the plates were infected with SARS-CoV-2 at 0.01 MOI and incubated for 1 h at 37 °C.

The inoculum was then removed and a volume of 2 mL of *A. annua* extract (100 μg/mL), EtOAc fraction (12.5–100 μg/mL), water fraction (100 μg/mL) and F2 (scopoletin, 50 μg/mL), F5 (arteannuin B, 50 μg/mL) and F8 (artemisinic acid, 50 μg/mL) were added to each infected well in triplicate. All the dilutions were prepared with medium. Untreated infected wells were used as a negative control (Ctrl) of the antiviral activity while remdesivir was used as a positive control.

The infected plates were left at 37 °C in a humidified 5% CO_2 atmosphere. After 24 h, the cytopathic effect (CPE) was observed, and each culture supernatant was collected for RNA extraction and virus titration for viral quantification. The RNAs extracted were tested by a TaqMan real-time RT- PCR (Bio-Rad) to target the SARS-CoV-2 N1 and N2 nucleocapsid genes, based on protocols developed by the Center for Disease Control and Prevention [40]. The 50% Tissue Culture Infectious Dose ($TCID_{50}$) assay was performed on the harvested samples to measure the viral titer as previously described [4,5]. Briefly, each supernatant (100 μL) was two-fold diluted in 96-well plates, and 22 000 cells/well in EMEM + 2% FCS were added (100 μL). Plates were left at 37 °C with 5% CO_2 for 6 days and checked daily to observe the cytopathic effect. The

50% end-point titers were determined using the Spearmane Karber method.

2.9. Surface plasmon resonance measurements

The isolated fractions that showed a virucidal activity against SARS-CoV-2 were tested to analyse their binding affinity to the viral proteins 3CLpro and S by Surface Plasmon Resonance (SPR). Binding studies were performed on Biacore X100 (Cytiva). 3CLpro was immobilized on a CM5 sensor chip by the amine coupling method as per manufacturer instructions by using acetate pH 5.0 and a final protein concentration of 50 μg mL^{-1} [41,42]. PBS-P (10 mM phosphate buffer, 150 mM NaCl, 0.05% surfactant P20) with 5% DMSO was used as a running and dilution buffer. Serial dilutions of the analytes were injected at 25 °C with a flow rate of 30 μL min^{1}. The surface was regenerated between samples with a 70% ethylene glycol solution. All data were zero adjusted and the reference (blank) was subtracted.

2.10. Antioxidant effect against reactive oxygen species (ROS)

To assess ROS generation, A549 cells were plated at a density of 1×10^4 cells/well on 96-well plates in a final volume of 100 μL/well. To induce oxidative stress, the TBH at 500 μM was used alone or in combination with 25, 50, 100, and 200 μg/mL of *A. annua* extract for 2 h. At the end of the treatment, each sample was added to 2′,7′-dichlorofluorescin diacetate at a final concentration of 1 mM (DCFH-DA, Merck, Darmstadt, Germany) and incubated in the dark at 37 °C for 30 min. After washing with PBS, the cells were analyzed by measuring the fluorescence intensity with a Microplate Reader GloMax fluorimeter (Promega Corporation, Madison, USA) at the excitation wavelength of 475 nm and emission wavelength of 530 nm. In addition, the cells were analyzed with a fluorescence microscope (Axio Scope 2 microscope; Zeiss, Oberkochen, Germany).

2.11. Statistical analysis

The statistical evaluation of the data was carried out using the GraphPad Prism 8.4.3 software (Northside Dr, San Diego, CA, USA). All the samples were analyzed three time independently and the values reported were obtained as the mean of at least three independent experiments ± standard errors (SE). Statistical evaluations were performed using one-way ANOVA followed by Tukey's Post hoc test. Differences in p-value of less than 0.01 were considered as statistically significant.

The IC_{50} value from the PRNT assay was calculated using GraphPad Prism version 9.0.0 (GraphPad Software, LLC., San Diego, USA) for Windows.

3. Results

3.1. Isolation of bioactive compounds

A preliminary identification of secondary metabolites from *A. annua* was conducted on a crude tincture by NMR heteronuclear correlation experiments, following a procedure recently reported by Kontogianni [43]. Through $^{1}H–^{13}C$ Heteronuclear Quantum Coherence (HSQC) and Multiple Bond Correlation (HMBC), we identified *A. annua* compounds in the dried tincture sample. The diagnostic cross peaks and the reference literature are summarized in Table 1. From the 2D experiments by HSQC and HMBC, it was possible to highlight the presence of characteristic signals of some secondary metabolites, such as flavonoids and artemisinin analogues. In particular, we had strong evidence of the presence of artemisinic acid and arteannuin B. The structural attribution was based on the identification of cross peak signals in the HSQC spectrum and the long-range connectivity in the HMBC experiment. In general, diagnostic signals were easily identified as they were not in overcrowded spectral regions.

The compounds were separated by preparative HPLC, and the individual fractions were analysed by NMR, which confirmed the structure attributions (Figs. 1–3).

Scopoletin (**F2**) was identified by the presence in the ^{1}H NMR spectrum of distinctive doublet signals of H(2) and H(3) with a coupling constant of 9.5 Hz, which is due to the double bond hydrogens in the lactone ring.

For arteannuin B (**F5**), diagnostic signals were the methylene signals C(13)-H(13) at 117.50 and 5.42 ppm and 6.13 ppm and four cross peaks with carbons 7, 6, 11 and 12 at 52.6, 81.2, 138.6 and 169.7 ppm, respectively. Artemisinic acid (**F8**) showed an H(13) signal at 5.52 and 6.41 ppm and four cross peaks with carbons 6, 7 11 and 12 at 38.0, 42.3, 142.3, 171.5 ppm, respectively.

Regarding flavonoids (**F3**), the diagnostic cross peaks in the HSQC spectrum of the *A. annua* extract were the signals of C(2')-H(2'), C(5')-H(5'), C(6')-H(6') and C(8)-H(8).

3.2. Effects of the A. annua extract on A549 cell viability

A dose-effect study was conducted on the cell viability of A549 lung epithelia cells treated with *A. annua* extract through an MTS assay. For this investigation, the following doses were tested: 25, 50, 100, and 200 μg/mL, for 24 h. The results shown in Fig. 4(A)-(B) evidenced that the *A. annua* extract did not induce any significant changes in cellular morphology and viability at the doses administrated.

3.3. Effects of the A. annua extract on cell viability impaired by TBH treatment

As a first step, we evaluated the oxidative agent TBH sensitivity using MTS and DCHF-DA assays on A549 lung epithelial cells. The dose-effect study shown in Fig. 5A andB indicated that the A549 cells treated with TBH at 500 μM induced a 40% reduction in cell viability (Fig. 5A) and an evident alteration of cell morphology (Fig. 5B). Furthermore, the administered doses induced a dose dependent production of ROS (Fig. 5C-D), indicated by the increase in fluorescence intensity analyzed by fluorimeter (Fig. 5C) and fluorescence microscopy (Fig. 5D). Based on these results, we chose the 500 μM concentration for the subsequent experiments.

To analyze whether the *A. annua* extract were able to protect A549 cells against ROS, we treated the cells with TBH (500 μM) in combination with increasing concentrations of the extracts after 24 h. As detected by the MTS assay, the extract were able to reduce the toxicity induced by TBH in a dose-dependent manner, reaching a viability value comparable to the control at a concentration of 100 and 200 μg/mL of the *A. annua* extract (Fig. 6A). The results were also confirmed by the microscopic analyses in which a significant recovery of TBH-induced altered cell morphology was observed (Fig. 6B). The analysis of the cell size indicates that the *A. annua* extract was able to recover the alteration in the size of the cell body induced by TBH (Fig. 6C).

3.4. Effect of A. annua extract on ROS production induced by TBH treatment

The capacity of the *A. annua* extract to reduce ROS generation induced by TBH was analyzed by DCFH-DA assay. The result was evaluated by fluorimeter analysis (Fig. 7A) and fluorescence microscopy observation (Fig. 7B), in which untreated (Ctrl) or cells treated with *A. annua* extract at different doses did not show any fluorescence, indicating that the *A. annua* extract did not induce oxidative stress. In contrast, the treatment with *A. annua* extract, in a dose-dependent manner, eliminated TBH-induced ROS production (Fig. 7A-B). The result suggests that the components of the *A. annua* extract, such as polyphenols and flavonoids, play a significant role as antioxidant agents.

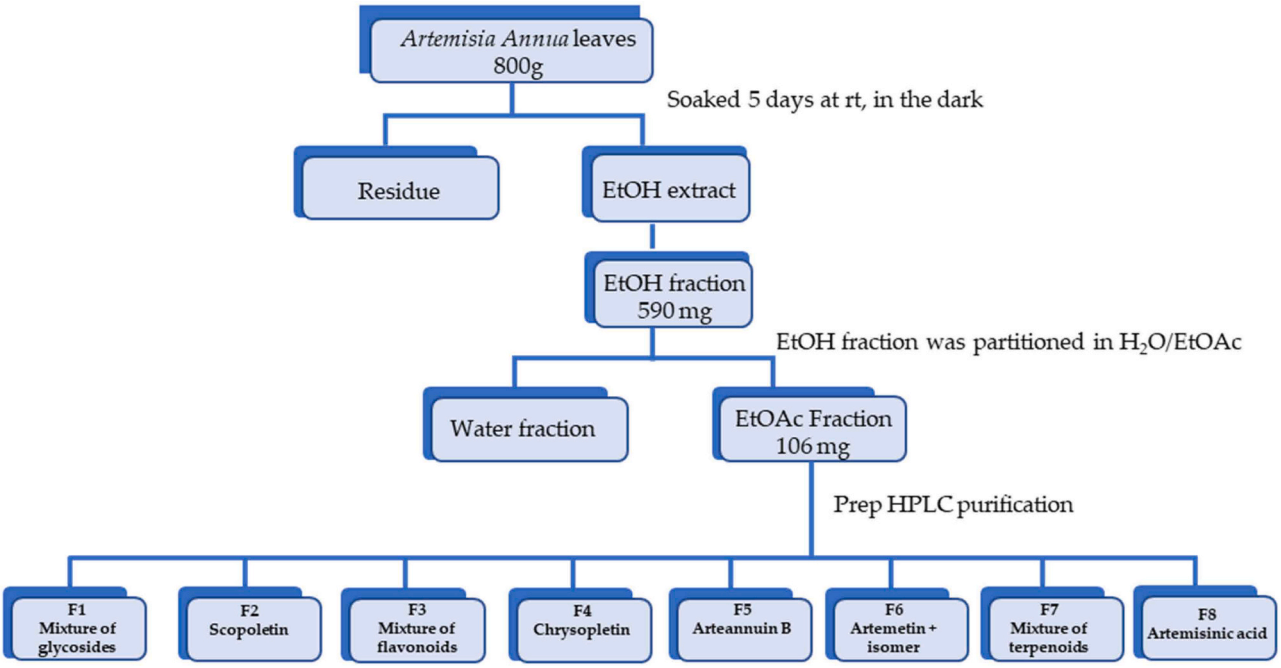

Fig. 1. *A. annua* extracts and isolated fractions.

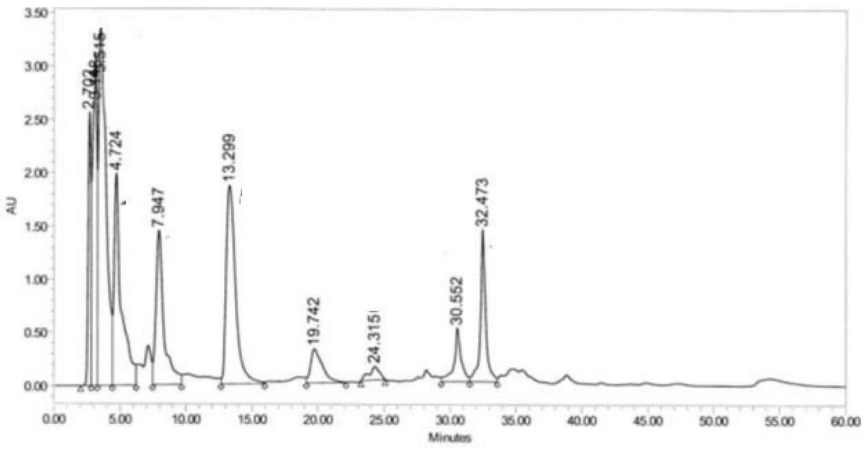

Fig. 2. HPLC fingerprint of the *A. annua* extract. The peak numbers refer to the fractions (1–8) reported in Table 1.

3.5. Cytotoxicity of the extracts on VERO E6 cell line

According to the results from the XTT assay, none of the dilutions of the *A. annua* extract showed a cytotoxic effect, as shown in Fig. 8A. EtOAc fraction was also tested by XTT: it showed a cytotoxic effect at a concentration of 1000 μg/mL, while lower concentrations (100 and 10 μg/mL) were not toxic.

All the isolated fractions (F1-F8) were tested at concentrations from 1 to 100 μg/mL (Fig. 8). Several fractions were cytotoxic at 100 μg/mL (OD ≤ 0,8). Scopoletin (F2), terpenoids (F7) and artemisinic acid (F8) were not toxic at any tested concentration.

3.6. Virucidal activity

The *A. annua* extract, which was serially diluted from 500 μg/mL to 0.0005 μg/mL, was tested to evaluate its virucidal activity on Vero E6 monolayers through the $PRNT_{50}$ method. As shown in Fig. 9A, the extract was effective against SARS-CoV-2 with an IC_{50} of 0.0015 μg/mL, calculated using a GraphPad Prism. Also, the EtOAc fraction was tested by $PRNT_{50}$ at concentrations ranging from 500 μg/mL to 0.0005 μg/mL: the results demonstrated that it was effective against SARS-CoV-2, with an IC_{50} of 0.00046 μg/mL.

The results of $PRNT_{50}$ on the water fraction at a concentration of 50 μg/mL showed a very low inhibition percentage (Fig. 9B), indicating that there was no virucidal effect.

The isolated fractions, F1–8, were also tested at a concentration of 50 μg/mL as reported in Fig. 9C: F2, F5–8 showed a significant virucidal activity (>80%), whereas fractions F1, F3 and F4 were less effective against the virus, however showing an activity > 60%.

3.7. Antiviral activity

The antiviral activity was measured by comparing the infection levels in infected Vero E6 cultures that were untreated and treated with *A. annua* extract, EtOAc fraction, water fraction, and selected single-compound fractions F2 (scopoletin), F5 (arteannuin B) and F8 (artemisinic acid), starting from the concentrations that showed the most virucidal activity (i.e., 50 μg/mL).

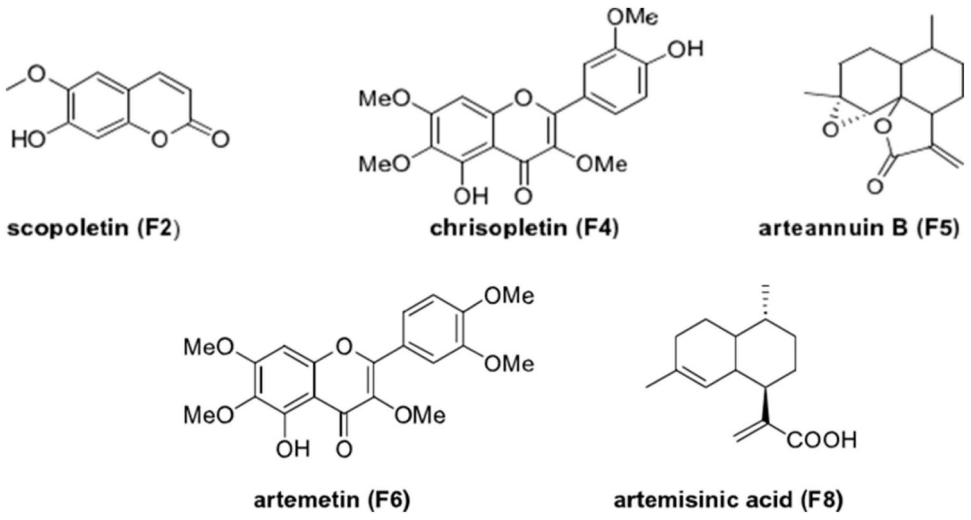

Fig. 3. Structures of isolated compounds compounds.

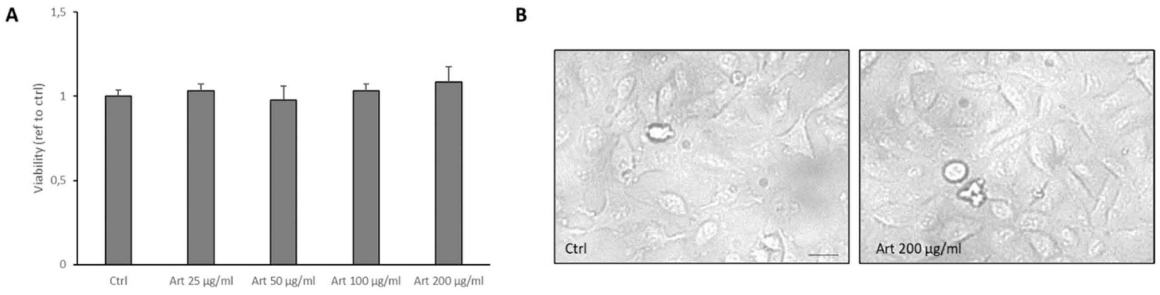

Fig. 4. Cytocompatibility of the *A. annua* extract. A: Cytotoxicity of the *A. annua* extract on A549 cells, by MTS assay; B: representative morphological images of untreated cells (Ctrl) and cells treated with 200 µg/mL of *A. annua* extract for 24 h. Scale Bar: 50 µm.

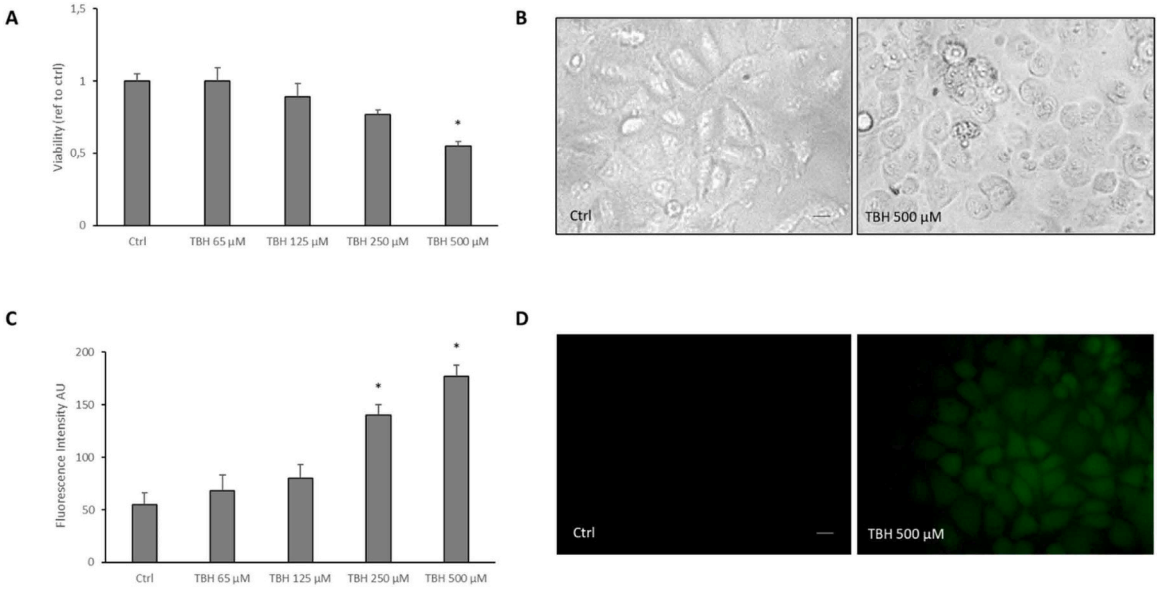

Fig. 5. Oxidative insult in A549 cells. A: Viability assay on untreated cells (ctrl) or cells treated with TBH at increasing concentrations; B: Representative morphological images of untreated cells (ctrl) or cells treated with TBH; C: Fluorescence intensity of untreated cells (Ctrl) and cells treated with TBH. (d) Fluorescence microscopy images of untreated cells (Ctrl) and cells treated with TBH. Scale Bar: 50 µm. Tukey test: $p < 0.01$ compared to Ctrl group.

The viral titer used for the infections was of $10^{7.9}$ $TCID_{50}$/mL, like the quantification of the SARS-CoV-2 control shown in Fig. 10A. The results showed that the *A. annua* and EtOAc fraction, F2, F5 and F8 all had an antiviral effect on the infected cells at 24 h p.i. with viral titres decreasing up to 10^{2} $TCID_{50}$/mL (EtOAc 50 µg/mL). In particular, the *A. annua* extract showed a mild activity at a concentration of 100 µg/mL

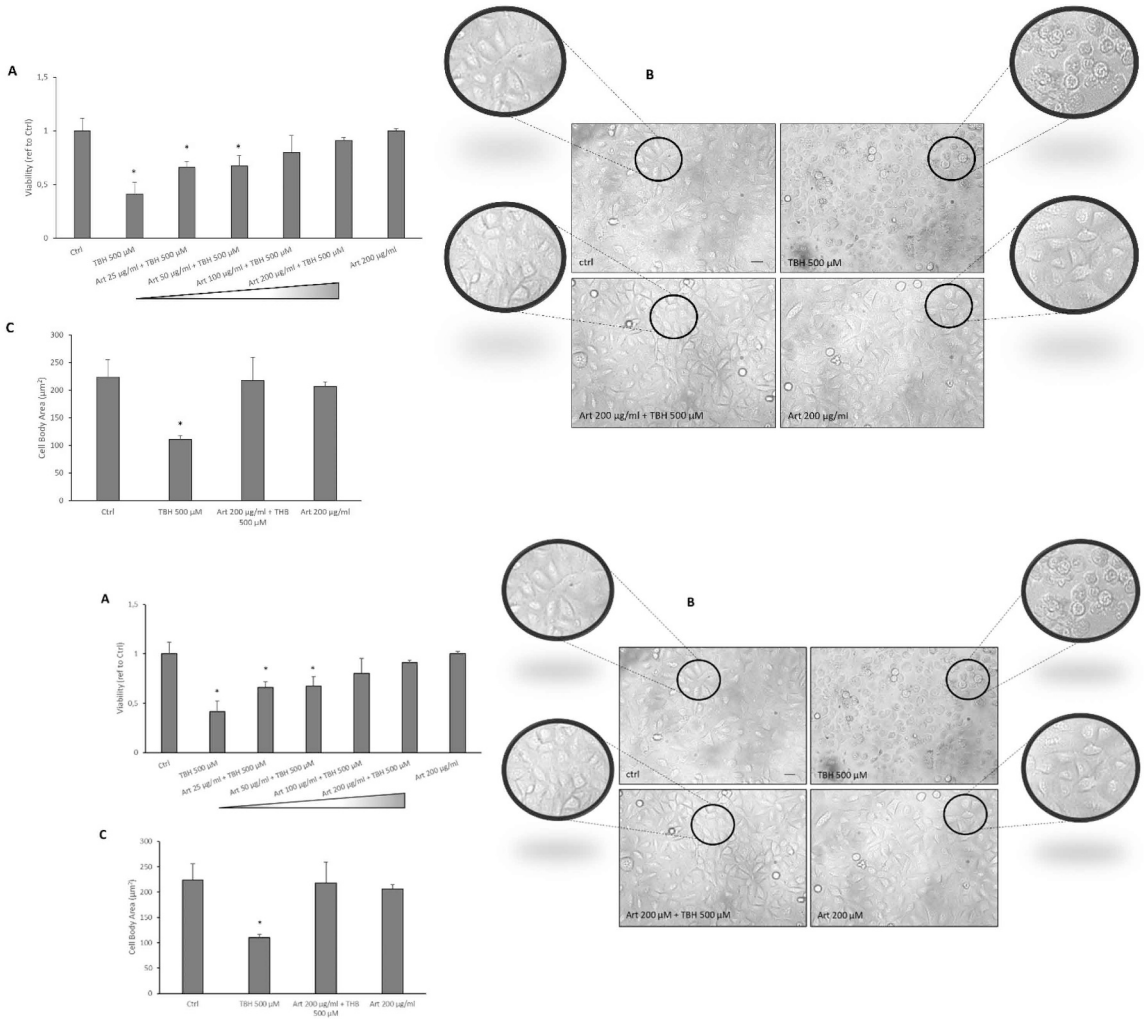

Fig. 6. *A. annua* extract protects A549 cells from oxidative damage. A: Viability assay on untreated cells (ctrl) or cells treated with TBH or cotreated with TBH and *A. annua* extract at increasing concentrations; B: Representative morphological images of untreated cells (Ctrl) or cells treated with TBH or cotreated with TBH and *A. annua* extract and treated with the *A. annua* extract alone; C: Histogram of cell body area of untreated cells (Ctrl) treated or with TBH alone or in combination with *A. annua* extract. Scale Bar: 50 µm. Tukey test: * $p < 0.01$ compared to ctrl group.

with a viral titer of $10^{6.2}$ $TCID_{50}$/mL. Interestingly, the EtOAc fraction maintained considerable activity down to a concentration of 12.5 µg/mL, whereas the isolated fractions F2, F5 and F8 were highly active down to 25 µg/mL. This effect was confirmed by the $TCID_{50}$ assay and the Real Time RT-PCR: the supernatants harvested from the treated wells showed a considerable decrease in the viral titer and in the amplification of SARS-CoV-2 N1 and N2 nucleocapsid genes, when compared with the supernatants harvested from untreated wells (Fig. 10A-B). In the assays above, the results confirmed the ineffectiveness of the water fraction at 100 µg/mL.

3.8. SPR measurements

The activity of the fractions F2 (scopoletin), F5 (arteannuin B)and F8 (artemisinic acid) was further investigated by immobilizing two proteins, Spike and 3CLpro, involved in two distinct phases of the viral cycle, namely, insertion and replication in the host cell. Scopoletin (Fig. 11a,b) showed a notable interaction with the Spike protein with a K_D value of $2.2{\cdot}10^{-4}$ M. Artemisinic acid formed a complex of equal intensity with the Spike protein (Fig. 11c, d). Notably, only the artemisinic acid (F8) and arteannuin B (F5) (Fig. 11e, f, g, h) formed a complex with 3CLpro at a lower concentration than mM, with a K_D value of $1.76{\cdot}10^{-4}$ M and $1.87{\cdot}10^{-4}$ M, respectively. These data suggest that the compounds may interfere with the viral pathways during the insertion and the replication process.

4. Discussion

Over the centuries, medicinal herbs have been used as treatment and as a preventive strategy for several diseases, including respiratory viral infections [44,45]. The benefit of using these herbs in viral respiratory infections is mainly due to their immune stimulating and inflammation modulating effects. The WHO has estimated that about 65–80% of the world's healthcare involves the use of traditional medicine to treat infectious diseases [46]. Several in vitro and in vivo studies carried out on plants and their derived products have helped to develop effective antibiotic, antimitotic, and antiviral treatments. The failure of several conventional drugs against viral infections and the increasing incidence of specific viral resistance has generated more interest in plants as an alternative source of effective antiviral agents [47,48]. Although herbal treatments were successfully used to treat coronavirus infections during the SARS-CoV and MERS-CoV outbreaks, there have been few investigations regarding a possible cure for COVID-19 disease by using natural compounds, which have been mostly limited to in silico studies [49,45,50].

A. annua, which has been known since ancient times as a healing

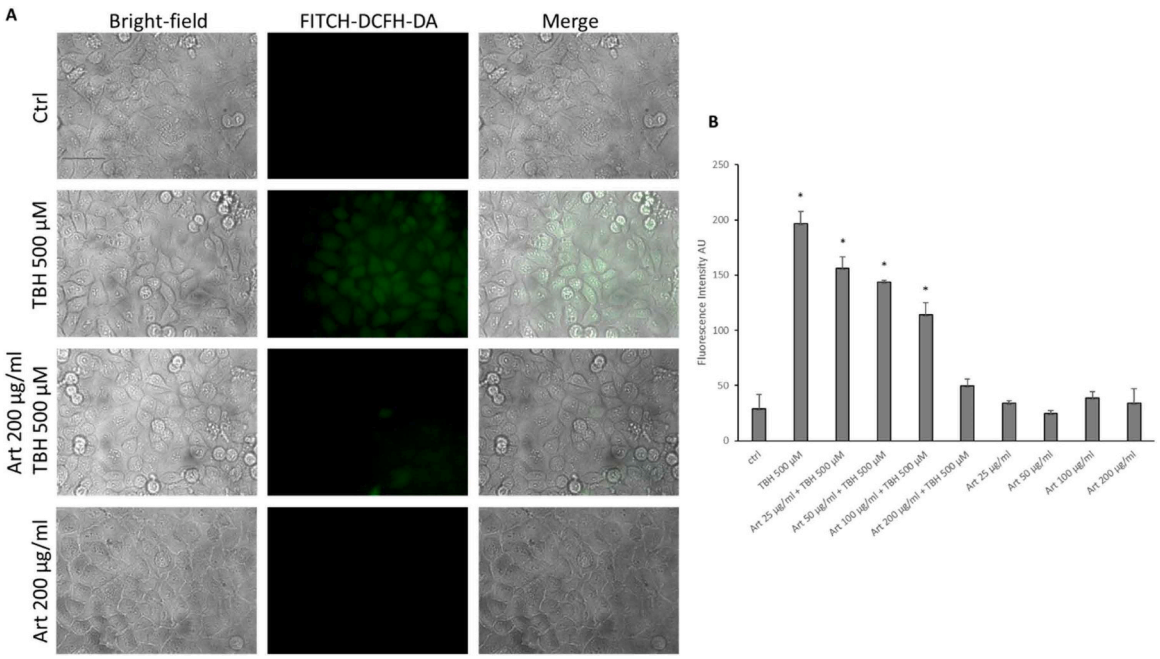

Fig. 7. *A. annua* extract protects A549 cells from oxidative insult. A: Fluorescence microscopy images of untreated cells (Ctrl) and cells treated with TBH or cotreated with TBH and *A. annua* extract; B: Fluorescence intensity of the treatment of untreated cells (Ctrl) or treated with the extract or with TBH alone or in combination with *A. annua* extract. Scale Bar: 50 µm. Tukey test: * $p < 0.01$ compared to ctrl group.

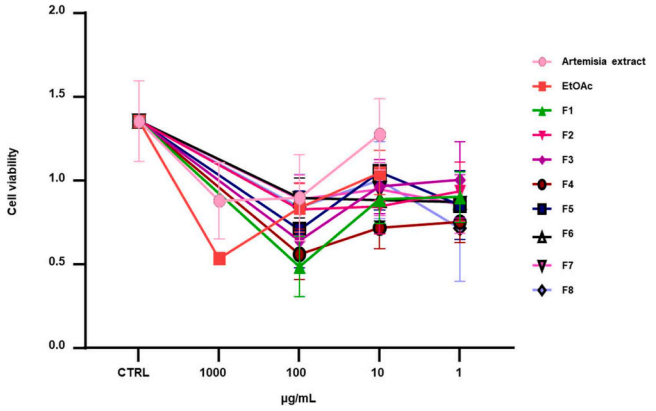

Fig. 8. Results of the XTT assay carried out to evaluate the viability of cells incubated with different concentrations of *A. annua* extract, EtOAc fraction and isolated components (F1-F8).

herb, has long intrigued researchers and healers. Its antimalarial properties were first demonstrated in the 1970 s during a Chinese military project, whose results led to the discovery that artemisinin, the active ingredient of the plant, kills the parasite that causes malaria. Artemisinin-based drugs, used in combination with other therapies according to WHO guidelines for the treatment of malaria, have helped reduce the mortality rate of malaria by more than 20%.

Artemisinin has been reported to have numerous pharmacological characteristics, including antiviral ones (Yuyong [24]). The broad-spectrum antiviral potential of Artemisia metabolites against a wide range of DNA and RNA viruses prompted us to investigate whether they could be used to combat COVID-19.

This study focused on the evaluation of the antioxidant, virucidal and antiviral potential of *A. annua* extracts against SARS-CoV-2 in vitro. In our first results, the crude extract showed virucidal and antioxidant effects in concentrations that do not affect cell viability. This extract also showed an antiviral effect, when used at a concentration of 100 µg/mL. Successively, the dried crude extract was partitioned between water and ethyl acetate. The aqueous fraction showed modest activity against the infected cells, whereas the EtOAc fraction and its isolated main components (F2, F5–8) exerted a considerable virucidal effect starting from a concentration of 50 µg/mL (Fig. 9). The effect was not observable when the infected cells were treated with other isolated fractions, i.e., F1, F3 and F4 (Fig. 9). The antiviral properties of the compounds that exerted a virucidal activity were demonstrated at concentrations that did not affect the growth of the cells. These results were also confirmed by Real-Time RT-PCR experiments (Fig. 10).

Among the isolated pure compounds, artemisinic acid showed the strongest virucidal and antiviral activity, thus it was selected to evaluate its interaction with the Spike and Mpro proteins using SPR. Previous studies reported that artemisinic acid could be a candidate drug for chronic urticaria due to the inhibitory effect on non-IgE-mediated passive skin anaphylaxis in mice. This activity is exerted by inhibiting the activity of mast cells in tissues [51] and as precursor of antimalaric Artemisinin [52]. We also investigated scopoletin, intrigued by recent in silico studies by Ikanovich et al. (2021) that predicted a significant binding affinity of the compound to the SARS-CoV-2 Mpro. We demonstrated that both scopoletin and artemisinic acid have a strong interaction with the viral protein Spike. Moreover, artemisinic acid and arteannuin B are able to effectively interact with 3CLpro (Fig. 11) showing a possible synergic effect. A limitation of this study is that we tested the antiviral activity of A. annua activities only against the wild type strain of SARS-CoV-2 that was circulating in 2020 in Italy. However, flavonoids are active against different viral diseases, and perform their antiviral activity by targeting the viral infections at multiple stages [53,54]. Recent studies, furthermore, reported antiviral activities of extracts of A. annua against the newest virus variants of SARS-CoV-2 [27,28].

5. Conclusions

Overall, our data confirm the antiviral, virucidal and antioxidant properties of the extract of A. annua against SARS-CoV-2. Moreover, for the first time, we demonstrate that artemisinic acid has a virucidal effect and a strong antiviral activity down to a concentration of 25 µg/mL. In

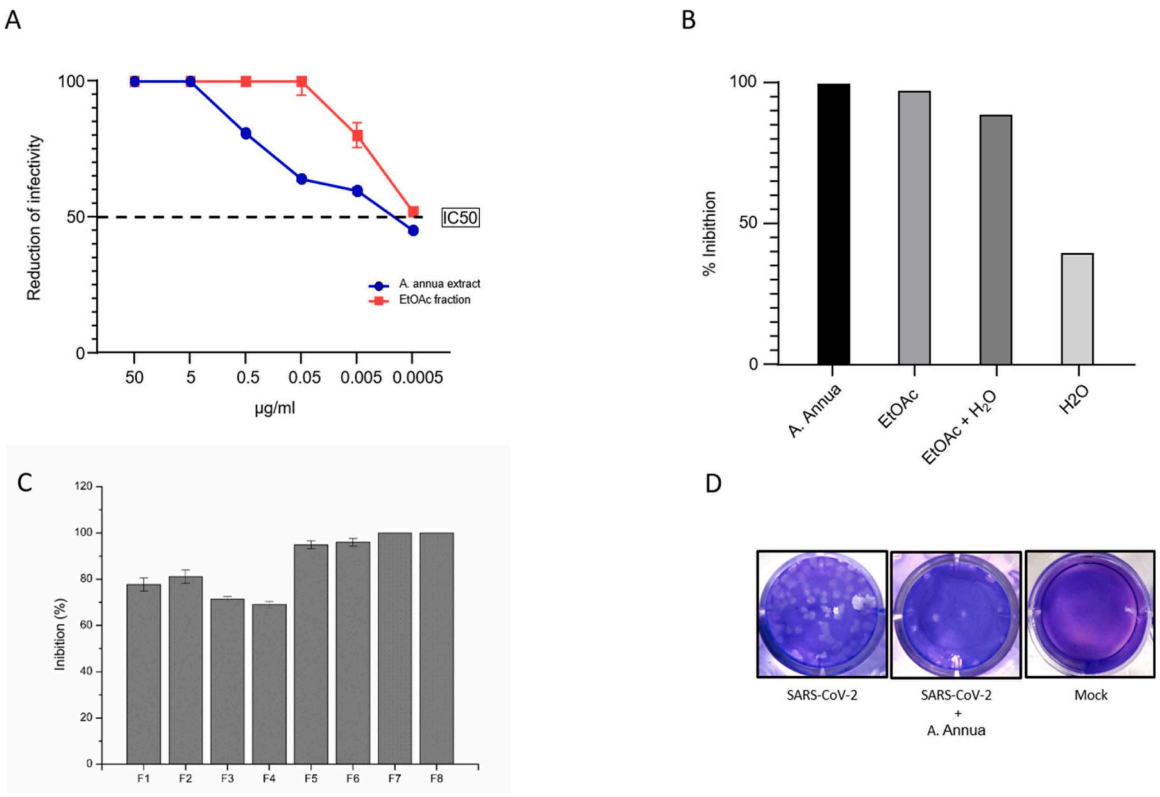

Fig. 9. A: Inactivation of SARS-CoV-2 by *A. annua* extract and EtOAc fraction. Half-maximal inhibitory concentration threshold, IC_{50}, is shown: *A. annua* extract was effective against SARS-CoV-2 down to a concentration of 0.005 µg/mL with an IC_{50} value of 0.0015 µg/mL; EtOAc fraction showed an IC_{50} value of 0.00046 µg/mL. B: Results of the virucidal activity of *A. annua* extract, the EtOAc fraction, the water fraction at the single concentration of 50 µg/mL, measured according to the percentage of viral inhibition. C: Inhibition of SARS-CoV-2 by *A. annua* single isolated fractions (F1-F8); D: SARS-CoV-2 plaques after fixing and staining with crystal violet at 3 days p.i.

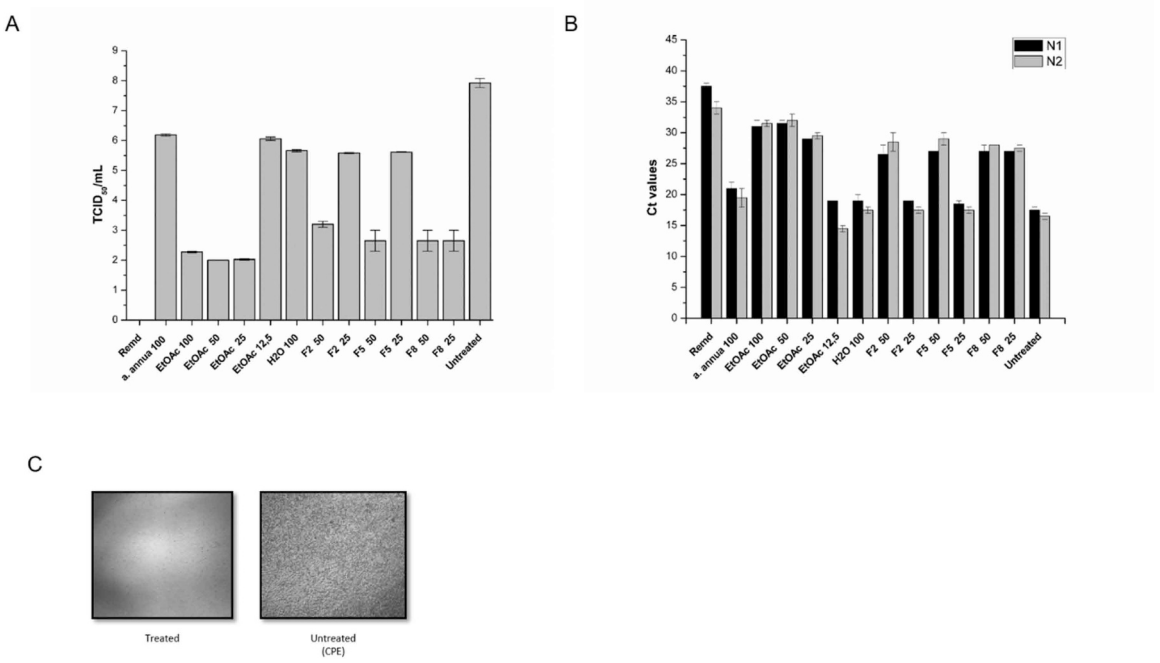

Fig. 10. A: Results of the $TCID_{50}$ assay performed on supernatants collected from Vero E6 cultures infected with SARS-COV-2 and treated with *A. annua* extract (ART), EtOAc fraction (EtOAc), water fraction, and single fractions F2 (scopoletin), F5 (arteannuin B) and F8 (artemisinic acid) at different concentrations (µg/mL). Viral titers were compared to the ones of untreated wells (SARS-CoV-2) and wells treated with Remdesivir (used as a positive control). B: Results of Real time RT-PCR on the RNAs extracted from each culture supernatant according to Ct values. Results of Real time RT-PCR according to Ct values of SARS-CoV-2 N1 and N2 nucleocapsid gene targets (mean of triplicates) on supernatants, harvested 24 h p.i., of treated and untreated Vero E6 cultures. Remdesivir was used as a positive control of the assay. C: CPE observed in wells treated and untreated.

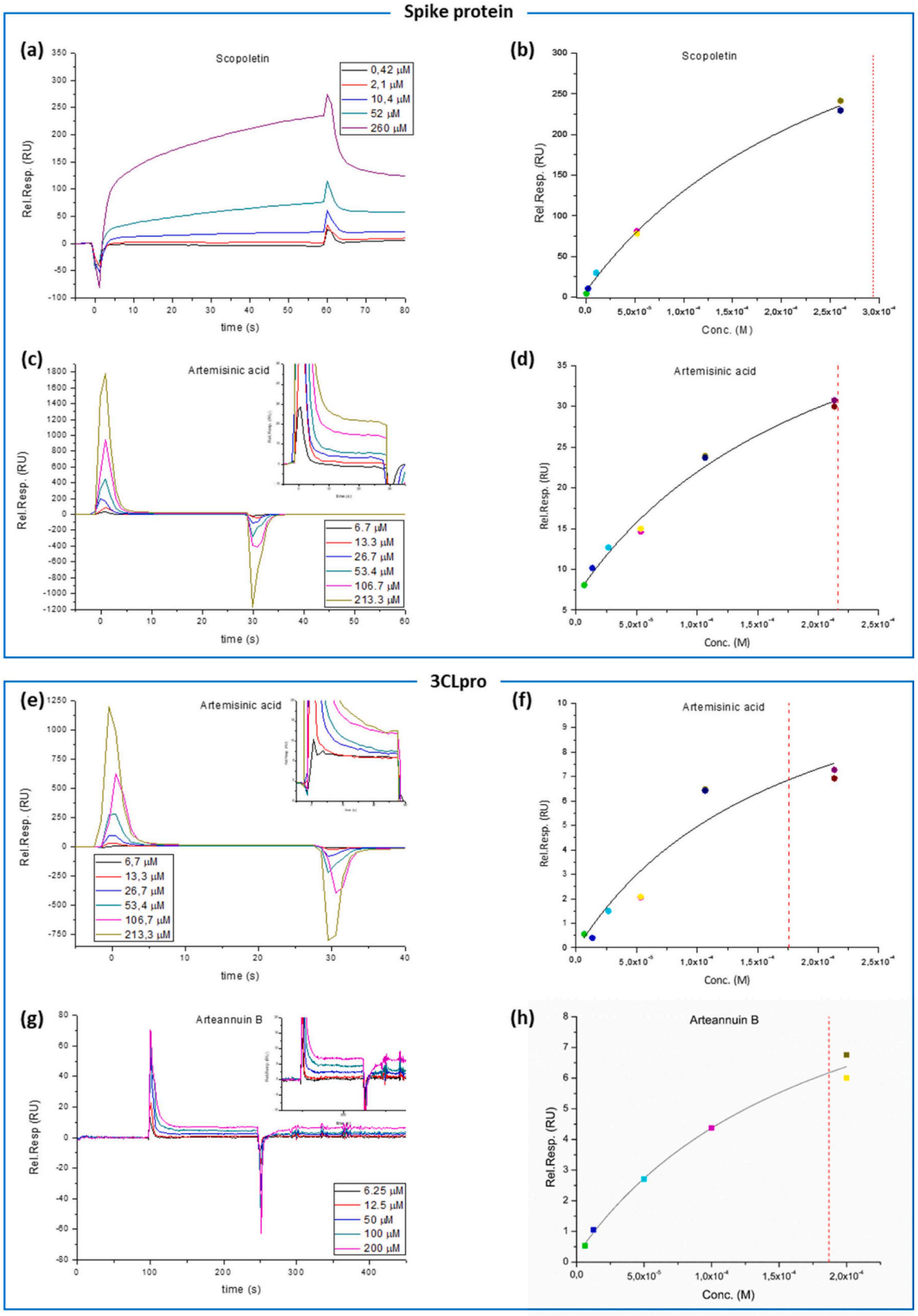

Fig. 11. SPR sensorgrams of scopoletin (a) and artemisinic acid (c) interactions with the Spike protein and relative affinity plots (b and d, respectively). *bottom*: sensorgrams (e, g) and affinity plot (f, h) of artemisinic acid and arteannuin B and 3CLpro. *(c,e) insets*: magnification of the association phase.

this work, we also evidenced that the inhibition of viral replication by artemisinic acid could be attributable to the inhibition of both the main protease, 3CLpro, and the Spike protein.

Investigation of the single main components of the extract showed artemisinic acid was a promising natural antiviral compound that is worth investigating further also to evaluate potential synergistic effects with other promising compounds such as scopoletin and arteannuin B.

In conclusion, our study evidenced the potential virucidal and antiviral activity of the *A. annua* crude extract and enriched fractions for the treatment of COVID-19The next step will be the validation of A. annua fractions against SARS-CoV-2 in an animal model. We look forward to, the publication of the results of the WHO COVID-19 Solidarity Therapeutics Plus Trial [55,56] clinical trials on the semi-synthetic A. annua derivative artesunate and we trust that our data could further improve the effective of these therapies.

Finally, the data that emerged from our study suggest that natural extract of A. annua and their components could have a key role as antioxidant and antiviral agents and support the fight against SARS-CoV-2 variants and other possible emerging Coronaviruses.

CRediT authorship contribution statement

Conceptualization: **F. Magurano, D. Nuzzo, A. Pinto**, Formal analysis and Investigation: **F. Magurano, M. Baggieri, S. Gioacchini, D. Nuzzo, P. Picone, R. Fioravanti, P. Bucci, M. Kojouri, G. Borgonovo, G. Catinella, S. Vasto, M. Retini, E. D'Ugo, A. Marchi, F. Ubaldi, S. Dallavalle**. Data curation and Writing – original draft: **F. Magurano, D. Nuzzo, M. Baggieri, S. Gioacchini, R. Fioravanti, A. Marchi, A. Pinto**, Writing – review & editing: **F. Magurano, D. Nuzzo, A. Pinto**, Approval of the version of the manuscript to be published: **F. Magurano, M. Baggieri, S. Gioacchini, D. Nuzzo, P. Picone, R. Fioravanti, P. Bucci, M. Kojouri, G. Borgonovo, G. Catinella, S. Vasto, R. Giuseppetti, E. D'Ugo, A. Marchi, F. Ubaldi, S. Dallavalle, A. Pinto**.

Declaration of Competing Interest

The authors declare that they have no known competing financial interests or personal relationships that could have appeared to influence the work reported in this paper.

Acknowledgments

This research was supported by EU funding within the MUR PNRR Extended Partnership initiative on Emerging Infectious Diseases (Project no. PE00000007, INF-ACT)". D.N. and P.P wish to acknowledge the "One Health Basic and Translational Research Actions addressing Unmet Needs on Emerging Infectious Diseases PE00000007" project, funded under the National Recovery and Resilience Plan, Mission 4 Education and Research - Component 2 From research to business - Investment 1.3, " Partenariati estesi alle Università, ai Centri di Ricerca, alle aziende per il finanziamento di progetti di ricerca di base" funded by the EU – NextGenerationEU"- D.D. MUR of concession Prot.n. 0001554 of 11/10/2022. A.P., S.D. and G.B. wish to acknowledge the project "One Health Action Hub: University Task Force for the resilience of territorial ecosystems" supported by Università degli Studi di Milano –PSR 2021 -GSA -Linea 6.

References

[1] WHO. Weekly Epidemiological Update on COVID-19 - 22 February 2023.
[2] M. Wang, R. Cao, L. Zhang, X. Yang, J. Liu, M. Xu, Z. Shi, Z. Hu, W. Zhong, G. Xiao, Remdesivir and chloroquine effectively inhibit the recently emerged novel coronavirus (2019- nCoV) in vitro, Cell Res. 30 (2020) 269–271.
[3] A. Gajewski, A. Kośmider, A. Nowacka, O. Puk, M. Wiciński, Potential of herbal products in prevention and treatment of COVID-19. Literature review (Nov), Biomed. Pharm. 143 (2021), 112150, https://doi.org/10.1016/j.biopha.2021.112150.
[4] F. Magurano, M. Baggieri, A. Marchi, G. Rezza, L. Nicoletti, COVID-19 study group. SARS-CoV-2 infection: the environmental endurance of the virus can be influenced by the increase of temperature, Clin. Micro-Biol. Infect. 27 (2021) 289.e5–289.e7.
[5] F. Magurano, M. Sucameli, P. Picone, M. Micucci, M. Baggieri, A. Marchi, P. Bucci, S. Gioacchini, G. Catinella, G. Borgonovo, S. Dallavalle, D. Nuzzo, A. Pinto, Antioxidant activity of citrus limonoids and investigation of their virucidal potential against SARS-CoV-2 in cellular models, Nov 10, Antioxidants 10 (11) (2021) 1794, https://doi.org/10.3390/antiox10111794.
[6] F. Magurano, M. Micucci, D. Nuzzo, M. Baggieri, P. Picone, S. Gioacchini, R. Fioravanti, P. Bucci, M. Kojouri, M. Mari, M. Retini, R. Budriesi, L.B. Mattioli, I. Corazza, V. Di Liberto, L. Todaro, R. Giuseppetti, E. D'Ugo, A. Marchi, M. Mecca, M. D'Auria, A potential host and virus targeting tool against COVID-19: Chemical characterization, antiviral, cytoprotective, antioxidant, respiratory smooth muscle relaxant effects of Paulownia tomentosa Steud, ISSN 07533322, M Biomed. Pharmacother. Volume 158 (2023), 114083, https://doi.org/10.1016/j.biopha.2022.114083.
[7] P. Picone, T. Sanfilippo, R. Guggino, L. Scalisi, R. Monastero, R. Baschi, V. Mandalà, L. San Biagio, M. Rizzo, D. Giacomazza, C. Dispenza, D. Nuzzo, Neurological consequences, mental health, physical care, and appropriate nutrition in long-COVID-19, Sep 14, Cell Mol. Neurobiol. (2022) 1–11, https://doi.org/10.1007/s10571-022-01281-w.
[8] D. Nuzzo, G. Presti, P. Picone, G. Galizzi, E. Gulotta, S. Giuliano, C. Mannino, V. Gambino, S. Scoglio, M. Di Carlo, Effects of the Aphanizomenon flos-aquae Extract (Klamin®) on a Neurodegeneration Cellular Model, in: Oxid Med. Cell Longev, 2018, 2018, p. 9089016, https://doi.org/10.1155%2F2018%2F9089016.
[9] A. Scurria, M. Sciortino, A. Presentato, C. Lino, E. Piacenza, et al., Volatile compounds of lemon and grapefruit integroPectin, Molecules 26 (1) (2021) 51, https://doi.org/10.3390/molecules26010051.
[10] D.H.J. Cheong, D.W.S. Tan, F.W.S. Wong, T. Tran, Anti-malarial drug, artemisinin and its derivatives for the treatment of respiratory diseases, Pharmacol. Res. 158 (2020), 104901.
[11] W.E. Ho, H.Y. Peh, T.K. Chan, W.S. Wong, Artemisinins: pharmacological actions beyond anti-malarial, Pharm. Ther. 142 (1) (2014) 126–139, https://doi.org/10.1016/j.pharmthera.2013.12.001. Epub 2013 Dec 6. PMID: 24316259.
[12] Y. Tu, The development of new antimalarial drugs: qinghaosu and dihydroqinghaosu, Chin. Med. J. 112 (11) (1999) 976–977 (Nov).
[13] T. Uzun, O. Toptas, Artesunate: could be an alternative drug to chloroquine in COVID-19 treatment?, May 28, Chin. Med 15 (2020) 54, https://doi.org/10.1186/s13020-020-00336-8.
[14] A. Septembre-Malaterre, M.L. Rakoto, Marodon, Y. Bedoui, J. Nakab, E. Simon, L. Hoarau, S. Savriama, D. Strasberg, P. Guiraud, J. Selambarom, F. Gasque, *Artemisia annua*, a traditional plant brought to lightInt, J. Mol. Sci. 21 (2020) 4986, https://doi.org/10.3390/ijms21144986.
[15] A.D. Fuzimoto, An overview of the anti-SARS-CoV-2 properties of *Artemisia annua*, its antiviral action, protein-associated mechanisms, and repurposing for COVID-19 treatment, J. Integr. Med. 19 (5) (2021) 375–388, https://doi.org/10.1016/j.joim.2021.07.003. Epub 2021 Jul 22.
[16] S. Slezakova, J. Ruda-Kucerova, Anticancer activity of artemisinin and its derivatives (Nov), Anticancer Res 37 (11) (2017) 5995–6003, https://doi.org/10.21873/anticanres.12046.
[17] T. Efferth, Beyond malaria: the inhibition of viruses by artemisinin-type compounds, Biotechnol. Adv. 36 (2018) 1730–1737.
[18] M. Gendrot, I. Duflot, M. Boxberger, O. Delandre, P. Jardot, M. Le Bideau, et al., Antimalarial artemisinin-based combination therapies (ACT) and COVID-19 in Africa: in vitro inhibition of SARS-CoV2 replication by mefloquine-artesunate, Int. J. Infect. Dis. 99 (2020) 437–440, https://doi.org/10.1016/j.ijid.2020.08.032.
[19] T. Efferth, M.R. Romero, D.G. Wolf, T. Stamminger, J.J. Marin, M. Marschall, The antiviral activities of artemisinin and artesunate, Sep 15, Clin. Infect. Dis. 47 (6) (2008) 804–811, https://doi.org/10.1086/591195. PMID: 18699744.11.
[20] T. Efferth, M.R. Romero, D.G. Wolf, T. Stamminger, J.J. Marin, M. Marschall, The antiviral activities of artemisinin and artesunate, Sep 15, Clin. Infect. Dis. 47 (6) (2008) 804–811, https://doi.org/10.1086/591195.
[21] A. Flobinus, N. Taudon, M. Desbordes, B. Labrosse, F. Simon, M.C. Mazeron, N. Schnepf, Stability and antiviral activity against human cytomegalovirus of artemisinin derivatives (Jan), J. Antimicrob. Chemother. 69 (1) (2014) 34–40, https://doi.org/10.1093/jac/dkt346. Epub 2013 Sep 3.
[22] S. Li, C. Chen, H. Zhang, G. Hy, H. Wang, L. Wang, P.G. Xiao, Identification of natural compounds with antiviral activities against SARS-associated coronavirus, Antivir. Res 67 (2005) 18–23, https://doi.org/10.1016/j.antiviral.2005.02.007.
[23] Y. Han, H.T. Pham, H. Xu, Y. Quan, T. Mesplède, Antimalarial drugs and their metabolites are potent Zika virus inhibitors, J. Med. Virol. 91 (7) (2019) 1182–1190, https://doi.org/10.1002/jmv.25440. Epub 2019 Mar 4.
[24] Y. Zhou, K. Gilmore, S. Ramirez, et al., In vitro efficacy of artemisinin-based treatments against SARS-CoV-2, Published 2021 Jul 16, Sci. Rep. 11 (1) (2021) 14571, https://doi.org/10.1038/s41598-021-93361-y.
[25] R. Cao, H. Hu, Y. Li, X. Wang, M. Xu, J. Liu, H. Zhang, Y. Yan, L. Zhao, W. Li, T. Zhang, D. Xiao, X. Guo, Y. Li, J. Yang, Z. Hu, M. Wang, W. Zhong, Anti-SARS-CoV-2 potential of artemisinins in vitro, Sep 11, ACS Infect. Dis. 6 (9) (2020) 2524–2531, https://doi.org/10.1021/acsinfecdis.0c00522. Epub 2020 Aug 18.
[26] M.S. Nair, Y. Huang, D.A. Fidock, S.J. Polyak, J. Wagoner, M.J. Towler, P. J. Weathers, Artemisia annua L. extracts inhibit the in vitro replication of SARS-CoV-2 and two of its variants, J. Ethnopharmacol. 274 (2021), 114016, https://doi.org/10.1016/j.jep.2021.114016.

[27] M.S. Nair, Y. Huang, D.A. Fidock, M.J. Towler, P.J. Weathers, Artemisia annua L. hot-water extracts show potent activity in vitro against Covid-19 variants including delta, J. Ethnopharmacol. 284 (2022), 114797, https://doi.org/10.1016/j.jep.2021.114797.
[28] M.S. Nair, Y. Huang, M. Wang, P.J. Weathers, SARS-CoV-2 omicron variants are susceptible in vitro to Artemisia annua hot water extracts, J. Ethnopharmacol. 308 (2023), 116291, https://doi.org/10.1016/j.jep.2023.116291.
[29] R. Rolta, D. Salaria, P. Sharma, B. Sharma, V. Kumar, B. Rathi, M. Verma, A. Sourirajan, D.J. Baumler, K. Dev, Phytocompounds of Rheum emodi, Thymus serpyllum, and *Artemisia annua* Inhibit Spike Protein of SARS-CoV-2 Binding to ACE2 receptor: in silico approach, Curr. Pharm. Rep. 7 (4) (2021) 135–149, https://doi.org/10.1007/s40495-021-00259-4. Epub 2021 Jul 15.
[30] M. Sehailia, S. Chemat, Antimalarial-agent artemisinin and derivatives portray more potent binding to Lys353 and Lys31-binding hotspots ofSARS-CoV-2 spike protein than hydroxychloroquine: potential repurposing of artenimol for COVID-19, J. Biomol. Struct. Dyn. 39 (2020) 6184–6194, https://doi.org/10.1080/07391102.2020.1796809.
[31] F.M. Uckun, S. Saund, H. Windlass, V. Trieu, Repurposing anti-malaria phytomedicine artemisinin as a COVID-19 drug, Mar 19, Front Pharm. 12 (2021), 649532, https://doi.org/10.3389/fphar.2021.649532.
[32] Ikanovic T., Sehercehajic E., Saric B., Tomic N.,Hadziselimovic R. In Silico Analysis of Scopoletin Interaction with Potential SARS-CoV-2 Target. NT 2021, LNNS 233, pp. 897–903, 2021. ⟨https://doi.org/10.1007/978–3-030–75275-0_99⟩.
[33] Y. Song, K.T. Desta, G.S. Kim, S.J. Lee, W.S. Lee, Y.H. Kim, J.S. Jin, A.M. Abd El-Aty, H.C. Shin, J.H. Shim, S.C. Shin, Polyphenolic profile and antioxidant effects of various parts of *Artemisia annua* L, Biomed. Chromatogr. 30 (4) (2016) 588–595, https://doi.org/10.1002/bmc.358.
[34] E. Lo Presti, D. Nuzzo, W. Al Mahmeed, et al., Molecular and pro-inflammatory aspects of COVID-19: the impact on cardiometabolic health, Biochim. Et. Biophys. Acta - Mol. Basis Dis. 1868 (12) (2022), 166559, https://doi.org/10.1016/j.bbadis.2022.166559.
[35] D. Nuzzo, S. Vasto, L. Scalisi, S. Cottone, G. Cambula, M. Rizzo, et al., Post-acute COVID-19 neurological syndrome: a new medical challenge, J. Clin. Med. 10 (9) (2021) 1947, https://doi.org/10.3390/jcm10091947.
[36] D. Nuzzo, G. Cambula, I. Bacile, M. Rizzo, M. Galia, P. Mangiapane, P. Picone, D. Giacomazza, L. Scalisi, Long-term brain disorders in post covid-19 neurological syndrome (PCNS) patient, Brain Sci. 11 (4) (2021) 454, https://doi.org/10.3390/brainsci11040454.
[37] S. Golabi, S. Ghasemi, M. Adelipour, R. Bagheri, K. Suzuki, A. Wong, M. Seyedtabib, M. Naghashpour, Oxidative stress and inflammatory status in COVID-19 outpatients: a health center-based analytical cross-sectional study, Mar 22, Antioxidants 11 (4) (2022) 606, https://doi.org/10.1016/j.ijid.2020.08.032.
[38] A. Baetas, M. Arruda, Muller ACoumarins and alkaloids from the steams of Metrodorea Flavida, J. Braz. Chem. Soc. 10 (3) (1999) 181–183.
[39] P. Bhandari, A.P. Gupta, B. Singh, V.K. Kaul, Simultaneous densitometric determination of artemisinin, artemisinic acid and arteannuin-B in Artemisia annua using reversed-phase thin layer chromatography, J. Separat Sci. 28 (2005) 2288–2292, https://doi.org/10.1002/jssc.200500198.
[40] Centers of Disease Control and Prevention (CDC). 2019-Novel Coronavirus (2019-nCoV) Real-time rRTPCR Panel Primers and Probes. Updated: May 29, 2020.
[41] B. Chen, SPR biosensor as a tool for screening prion protein binders as potential anti prion leads, Methods Mol. Biol. 627 (2010) 147–155, https://doi.org/10.1007/978-1-60761-670-2_9.
[42] G.A. Papalia, S. Leavitt, M.A. Bynum, P.S. Katsamba, R. Wilton, H. Qiu, M. Steukers, S. Wang, L. Bindu, S. Phogat, A.M. Giannetti, T.E. Ryan, V.A. Pudlak, K. Matusiewicz, K.M. Michelson, A. Nowakowski, A. Pham-Baginski, J. Brooks, B. C. Tieman, B.D. Bruce, M. Vaughn, M. Baksh, Y.H. Cho, M.D. Wit, A. Smets, J. Vandersmissen, L. Michiels, D.G. Myszka, Comparative analysis of 10 small molecules binding to carbonic anhydrase II by different investigators using Biacore technology, Anal. Biochem. 359 (1) (2006) 94–105, https://doi.org/10.1016/j.ab.2006.08.021.
[43] V. Kontogianni, A. Primikyri, M.S. Ioannis, P. Gerothanassis, Simultaneous determination of artemisinin and its analogs and flavonoids in *Artemisia annua* crude extracts with the use of NMR spectroscopy, Magn. Reson. Chem. 58 (2020) 232–244, https://doi.org/10.1002/mrc.4971.
[44] G. Kiran, L. Karthik, M.S. Shree Devi, P. Sathiyarajeswaran, K. Kanakavalli, K. M. Kumar, In silico computational screening of Kabasura Kudineer-official Siddha Formulation and JACOM against SARSCoV-2 spike protein, J. Ayurveda Integr. Med. 25 (20) (2020) S0975–S9476, https://doi.org/10.1016/j.jaim.2020.05.009.
[45] M. Tahir Ul Qamar, S.M. Alqahtani, M.A. Alamri, L.L. Chen, Structural basis of SARS-CoV-2 3CLpro and antiCOVID-19 drug discovery from medicinal plants (Aug), J. Pharm. Anal. 10 (4) (2020) 313–319, https://doi.org/10.1016/j.jpha.2020.03.009.
[46] S.Y. Pan, G. Litscher, K. Chan, Z.L. Yu, H.Q. Chen, K.M. Ko, Traditional medicines in the world: where to go next? Evid. Based Complement Altern. Med. 2014 (2014), 739895 https://doi.org/10.1155/2014/739895. Epub 2014 Dec 29.
[47] M. Daglia, Polyphenols as antimicrobial agents (Apr), Curr. Opin. Biotechnol. 23 (2) (2012) 174–181, https://doi.org/10.1016/j.copbio.2011.08.007. Epub 2011 Sep 16.
[48] K.K. Irwin, N. Renzette, T.F. Kowalik, J.D. Jensen, Antiviral drug resistance as an adaptive process, Jun 10, Virus Evol. 2 (1) (2016) vew014, https://doi.org/10.1093/ve/vew014.
[49] L. Babaeekhou, M. Ghane, M. Abbas-Mohammadi, In silico targeting SARS-CoV-2 spike protein and main protease by biochemical compounds, Biologia 76 (11) (2021) 3547–3565, https://doi.org/10.1007/s11756021-00881-z. Epub 2021 Sep 22.
[50] P. Umadevi, S. Manivannan, A.M. Fayad, S. Shelvy, In silico analysis of phytochemicals as potential inhibitors of proteases involved in SARS-CoV-2 infection, J. Biomol. Struct. Dyn. 40 (11) (2022) 50535059, https://doi.org/10.1080/07391102.2020.1866669. Epub 2020 Dec 29.
[51] Ding, B. Dang, Y. Wang, C. Zhao, H. An, Artemisinic acid attenuated symptoms of substance P-induced chronic urticaria in a mice model and mast cell degranulation via Lyn/PLC-p38 signal pathway, Int. Immunopharmacol. 113 (2022), 109437.
[52] D.K. Ro, E.M. Paradise, M. Ouellet, K.J. Fisher, K.L. Newman, J.M. Ndungu, K. A. Ho, R.A. Eachus, T.S. Ham, J. Kirby, M.C. Chang, S.T. Withers, Y. Shiba, R. Sarpong, J.D. Keasling, Production of the antimalarial drug precursor artemisinic acid in engineered yeast, Apr 13, Nature 440 (7086) (2006) 940–943, https://doi.org/10.1038/nature04640.
[53] S.L. Badshah, S. Faisal, A. Muhammad, B.G. Poulson, A.H. Emwas, M. Jaremko, Antiviral activities of flavonoids (Aug), Biomed. Pharm. 140 (2021), 111596, https://doi.org/10.1016/j.biopha.2021.111596.
[54] E.V. LeBlanc, C.C. Colpitts, The green tea catechin EGCG provides proof-of-concept for a pan-coronavirus attachment inhibitor, Jul 28, Sci. Rep. 12 (1) (2022) 12899, https://doi.org/10.1038/s41598-022-17088-0.
[55] ISRCTN registry: ISRCTN18066414 https://doi.org/10.1186/ISRCTN18066414. SOLIDARITY TRIAL PLUS: An international randomized trial of additional treatments for COVID-19 in hospitalized patients who are all receiving the local standard of care. Submission date 20/04/2021. Registration date 29/07/2021.
[56] WHO COVID-19 Solidarity Therapeutics Trial (2021). Study website: ⟨https://www.who.int/emergencies/diseases/novel-coronavirus-2019/global-research-on-novel-coronavirus-2019-ncov/solidarity-clinical-trial-for-covid-19-treatments⟩.